Electronic Supplementary Material (ESI) for Materials Chemistry Frontiers.

Supporting Information

Carbonized polymer dots/TiO_2 photonic crystals heterostructures with enhanced light harvesting and charge separation for efficient and stable photocatalysis

Yue Zhao,‡ Qingsen Zeng,‡ Tanglue Feng, Chunlei Xia, Chongming Liu, Fan Yang, Kai Zhang, Bai Yang*

State Key Laboratory of Supramolecular Structure and Materials, College of Chemistry, Jilin University, Changchun, 130012, P. R. China.

*E-mail: byangchem@jlu.edu.cn

‡Yue Zhao and Qingsen Zeng contributed equally to this work.

Table S1 Visible light activated TiO_2 photonic crystal photocatalysts and their application in the degradation of organic pollutants.

Materials	Pore template	Photocatalytic application	Irradiation conditions	Improved properties	performance	Ref.
TiO_2 PCs films	270, 340, 460, 550 nm PS opals	MB degradation	500 W Xe lamp ($320 < \lambda < 800$ nm)	light harvesting	EF ~1.6	1
TiO_2 PCs films	202, 356, 548 nm PS opals	CV degradation	Solar AM 1.5 ($\lambda > 400$ nm)	light harvesting	EF~1.22 vs TiO_2 NCs	2
N-TiO_2 PCs films	400 nm PS opal	MB degradation	Halogen lamp ($\lambda > 400$ nm)	light harvesting	EF ~ 1.7 vs TiO_2 NCs EF ~ 1.26 vs disordered TiO_2	3
Mesoporous N-TiO_2 spheres	290 nm silica opal, PMMA inverse opal	RhB degradation	300 W Xe lamp ($\lambda > 400$ nm)	light harvesting	EF ~ 4.0 vs mesoporous TiO_2 spheres	4
Mesoporous N-TiO_2 PCs films	80 nm and 300 nm PS opals	MB degradation	Xe lamp AM 1.5G, 100 mW cm^{-2} ($400 < \lambda < 600$ nm)	light harvesting, MB absorption	EF~4.9 vs meso TiO_2 PCs	5
N-TiO_2 PCs films	450 nm PS opal	TC degradation	300 W Xe lamp, ($\lambda > 400$ nm)	light harvesting	EF~6.1 vs conventional TiO_2 PCs	6
NF-TiO_2 PCs films	215 and 460 nm PS opals	RhB degradation	Xe lamp, AM 1.5G Natural sunlight	light harvesting	EF~1.6 vs NF-TiO_2 NCs	7
Ti^{3+} doped TiO_2 PCs films and powders	170, 265, 355 nm PS opals	AO7 degradation	500 W halogen lamp Hg lamp	light harvesting	EF~2.5 vs TiO_2 PCs	8
H-TiO_2 PCs films	360 nm PS opals	MB degradation	300 W Xe lamp ($\lambda > 400$ nm)	light harvesting	EF~1.35 vs white TiO_2 PCs	9
Pt-TiO_2 PCs films	185 nm PS opals	AO7 degradation	120 W Xe lamp, ($\lambda > 300$ nm)	Reaction activity	EF = 3.5-4.0, > 2 wt % Pt	10
TiO_2/Pt PCs films	120, 140, 193, 225 nm PS opals	phenol degradation	300 W Hg lamp 365 nm, 2.0 mW cm^{-2}	light harvesting, charge separation	EF~3.3 vs TiO_2 NCs	11
Au-TiO_2 PCs films	170 225, 257, 326, 398 nm PS opals	BA degradation	300 W Hg lamp ($\lambda > 340$ nm)	light harvesting, Reaction activity	EF~5.4 vs TiO_2 NCs	12
Au-TiO_2 PCs films	193 and 240 nm PS opals	2,4-DCP degradation	500 W Xe lamp, 100 mW cm^{-2} ($\lambda > 420$ nm)	light harvesting,	EF ~ 3.0 vs TiO_2 PCs	13
Ag-TiO_2 PCs films	315 nm SiO_2 spheres	MB degradation	$400 < \lambda < 760$ nm	light harvesting,	EF~ 1.48 vs TiO_2 PCs	14
Cu_2O-TiO_2 PCs films	260 and 193 nm PS opals	RhB and BPA degradation	300 W Xe lamp, 200 mW cm^{-2} ($320 < \lambda < 780$ nm)	light harvesting,	EFRhB~2.9, EFBPA~4.9 vs Cu_2O-TiO_2 NCs	15
ZnO-TiO_2 PCs films	300 nm PS opal	MO degradation	500 W Xe lamp ($320 < \lambda < 780$ nm)	charge separation	EF~1.9 vs ZnO-TiO_2 NCs	16
ZnO-TiO_2 PCs Powders	370 nm PS opal	RhB degradation	18 W Ne lamp ($\lambda > 400$ nm)	charge separation	EF~2.1 vs TiO_2 PCs EF~1.8 vs ZnO-TiO2	17
CPDs/TiO_2 PCs heterostructures	265 nm PS opal	MB degradation	Xe lamp AM 1.5G, 100 mW cm^{-2} ($\lambda > 420$ nm)	light harvesting, charge separation	EF ~ 2.0 vs TiO_2 PCs	This work

PCs: photonic crystals; EF: enhancement factor; NCs: nanocrystals.

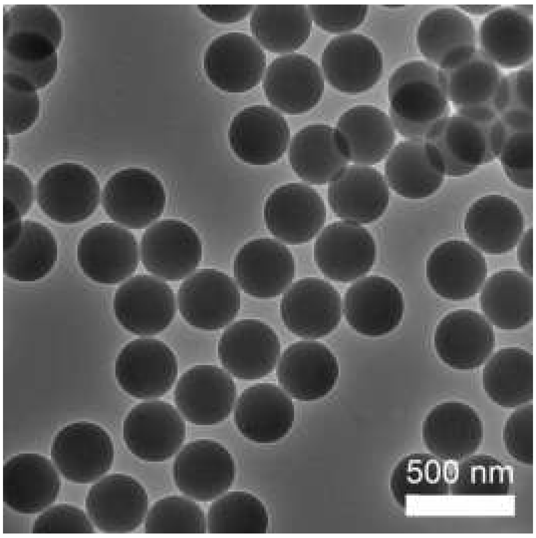

Figure S1 TEM image of as-prepared PS microspheres.

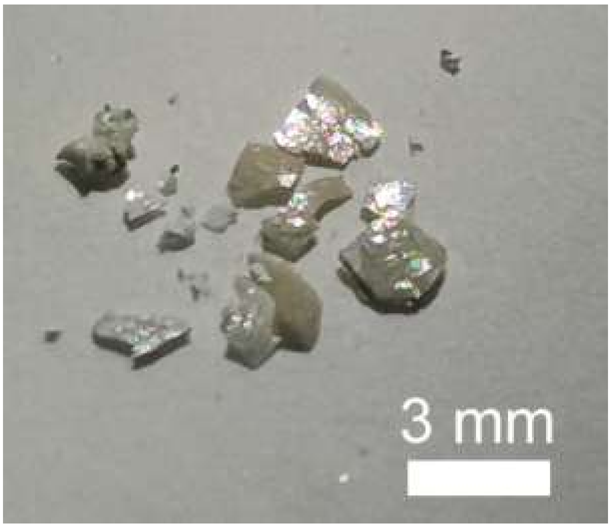

Figure S2 Optical image of as-prepared TiO_2 PCs powders, showing iridescent colors.

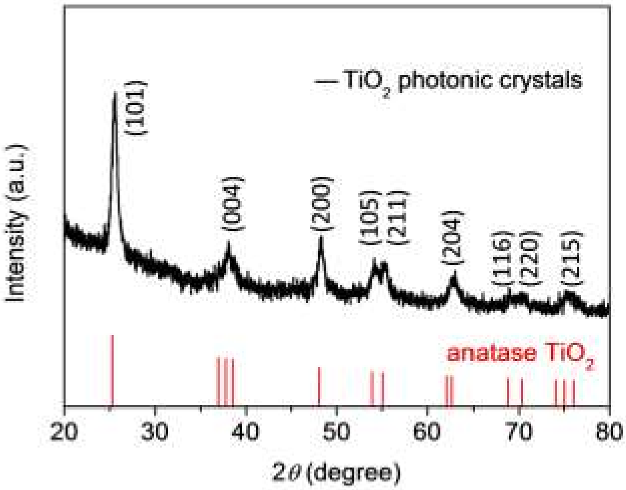

Figure S3 XRD patterns of TiO_2 PCs, whose crystalline phase is anatase.

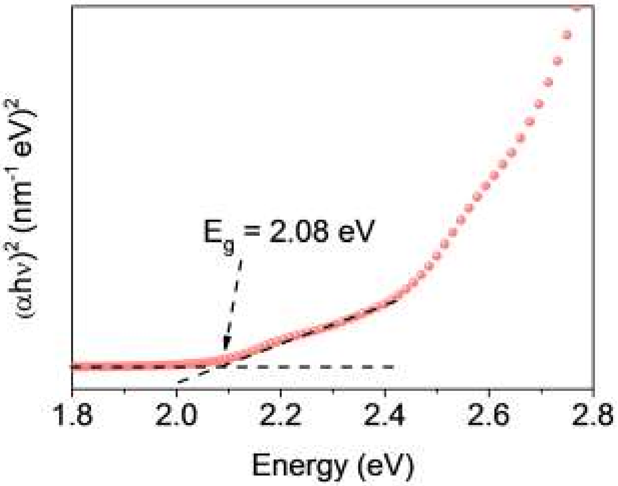

Figure S4 The plots of $(ah\nu)^2$ vs $h\nu$ calculated from absorption spectra of CPDs, indicating a E_g of 2.08 eV.

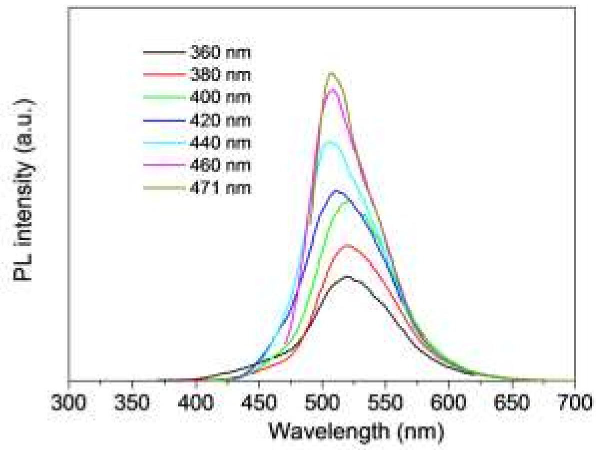

Figure S5 the CPDs PL spectra excited by excitation light with different wavelength.

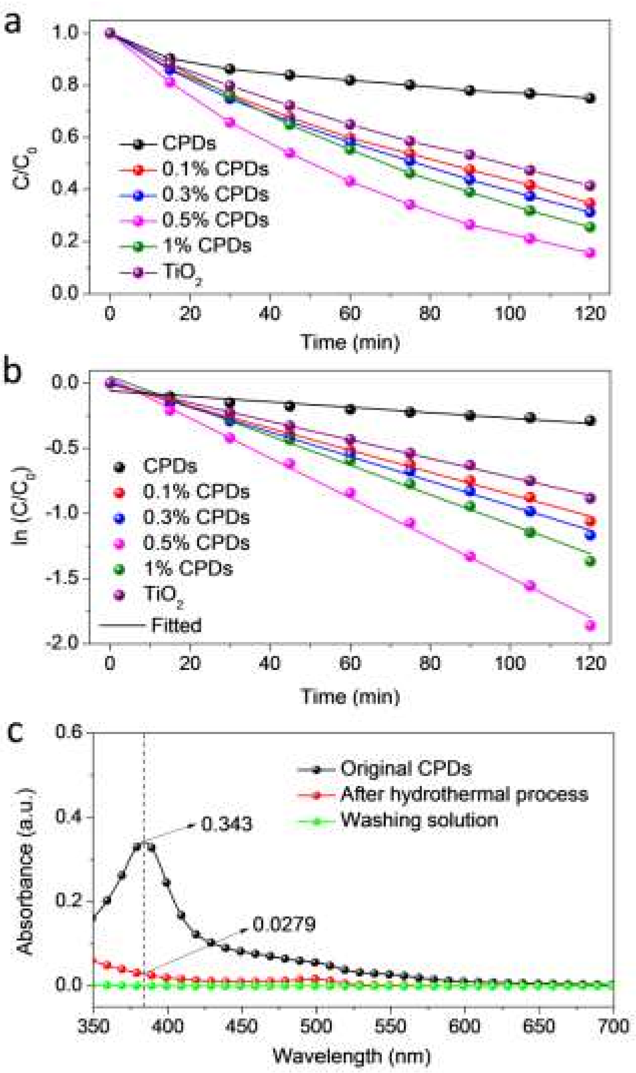

Figure S6 The optimization of CPDs content in CPDs/TiO_2 PCs heterostructures. (a) Evolution of relative concentration (C/C_0) of MB in different photocatalysts under one-sun visible light irradiation ($\lambda > 420$ nm). (b) $\ln(C/C_0)$ as a function of time. Nothing that the incorporation of CPDs can efficiently enhance the photocatalytic activity of TiO_2 PCs. When the content of CPDs reaches 0.5w%, the CPDs/TiO_2 PCs heterostructures exhibit the best catalytic activity. (c) The absorption spectra are used to monitor the actual loaded amount of CPDs onto TiO_2 PCs. Figure S4c is the absorption spectra of CPDs solution for preparing 1w% CPDs/TiO_2 PCs before (black curve) and after (red curve) hydrothermal reaction. Due to the extremely strong coordinating interaction between the TiO_2 PCs and polar groups of amino and carboxyl on CPDs, the absorption peaks located at 383 nm is almost disappeared with only 8.1% of its initial intensity after reacting with TiO_2 PCs, indicating a very high loaded proportion of 91.9% for CPDs. Furthermore, CPDs can't be washed away from the heterostructures during purification process (green curve). Therefore, the content of CPDs in the final heterojunction products is very close to the raw ratio. In addition, it is worth noting that the hydrothermal process for preparing CPDs/TiO_2 PCs is mild at only 140°C, which is much lower than the reaction temperature of synthesizing CPDs (200°C), so the changes of structure and absorption spectra for CPDs are negligible.

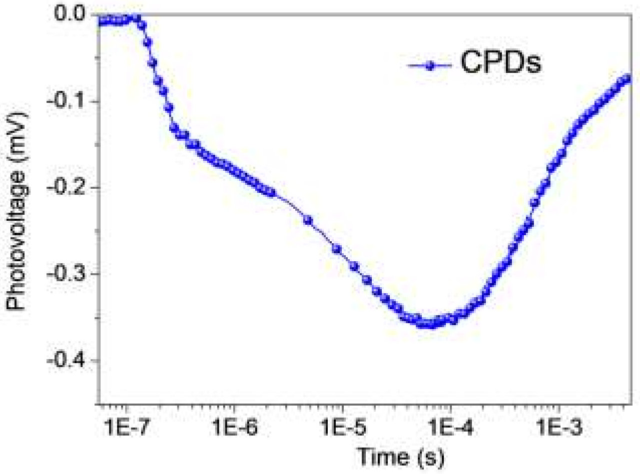

Figure S7 Transient photovoltage (TPV) curve of CPDs as a function of exponential time.

Reference

1. X. Zheng, S. Meng, J. Chen, J. Wang, J. Xian, Y. Shao, X. Fu and D. Li, *The Journal of Physical Chemistry C*, 2013, **117**, 21263-21273.
2. X. Zheng, D. Li, X. Li, L. Yu, P. Wang, X. Zhang, J. Fang, Y. Shao and Y. Zheng, *Physical chemistry chemical physics : PCCP*, 2014, **16**, 15299-15306.
3. Q. Li and J. K. Shang, *Journal of the American Ceramic Society*, 2008, **91**, 660-663.
4. Z. Hu, L. Xu and J. Chen, *Materials Letters*, 2013, **106**, 421-424.
5. S.-J. Ha, D. H. Kim and J. H. Moon, *RSC Advances*, 2015, **5**, 77716-77722.
6. Z. Hu, L. Xu, L. Wang, Y. Huang, L. Xu and J. Chen, *Catalysis Communications*, 2013, **40**, 106-110.
7. T. K. Rahul and N. Sandhyarani, *Nanoscale*, 2015, **7**, 18259-18270.
8. D. Qi, L. Lu, Z. Xi, L. Wang and J. Zhang, *Applied Catalysis B: Environmental*, 2014, **160-161**, 621-628.
9. L. Xin and X. Liu, *RSC Advances*, 2015, **5**, 71547-71550.
10. J. I. Chen, E. Loso, N. Ebrahim and G. A. Ozin, *Journal of the American Chemical Society*, 2008, **130**, 5420-5421.
11. H. Chen, S. Chen, X. Quan and Y. Zhang, *Environmental science & technology*, 2009, **44**, 451-455.
12. Z. Cai, Z. Xiong, X. Lu and J. Teng, *J. Mater. Chem. A*, 2014, **2**, 545-553.
13. Y. Lu, H. Yu, S. Chen, X. Quan and H. Zhao, *Environmental science & technology*, 2012, **46**, 1724-1730.
14. Y. Zhao, B. Yang, J. Xu, Z. Fu, M. Wu and F. Li, *Thin Solid Films*, 2012, **520**, 3515-3522.
15. Z. Geng, Y. Zhang, X. Yuan, M. Huo, Y. Zhao, Y. Lu and Y. Qiu, *Journal of Alloys and Compounds*, 2015, **644**, 734-741.
16. X. Zheng, D. Li, X. Li, J. Chen, C. Cao, J. Fang, J. Wang, Y. He and Y. Zheng, *Applied Catalysis B: Environmental*, 2015, **168**, 408-415.
17. M. Zalfani, B. van der Schueren, M. Mahdouani, R. Bourguiga, W.-B. Yu, M. Wu, O. Deparis, Y. Li and B.-L. Su, *Applied Catalysis B: Environmental*, 2016, **199**, 187-198.